# Improvement of a method for the characterization of ultrafiltration membranes by measurements of tracers retention

Christel Causserand, Sandrine Rouaix, Ahmad Akbari, Pierre Aimar

# Improvement of a method for the characterization of ultrafiltration membranes by measurements of tracers retention

C. Causserand*, S. Rouaix, A. Akbari, P. Aimar

*Laboratoire de Génie Chimique, CNRS/UPS/INP, UMR 5503, 118 route de Narbonne, 31062 Toulouse Cedex 04, France*

**Abstract**

The aim of this study is to improve protocols for assessing accurate characteristic retention curve and cut-off of membranes, thus enabling the manufacture and performance of the membrane to be monitored. Different data treatments are considered in order to determine membrane retention for fractions of tracer filtered (PEGs in the molar mass range of 1–100 kg mol$^{-1}$). In the most advanced method of treatment, the observed retention is expressed as a combination of solute transfer coefficients in the boundary layer ($k_{BL}$) and porous structure ($k_{pore}$), and the asymptotic retention ($R_{inf}$), which is an intrinsic characteristic of the membrane to solute as it is independent of operating conditions.

The developed method has proved to be accurate and reproducible in two cases: (i) monitoring of UF membrane integrity during accelerated aging; (ii) for quantification of cut-off change due to UF membrane modification by UV grafting. We propose a simplified procedure that allows a reduction in experimental workload, without loss of sensitivity, for the most advanced method.

*Keywords:* Ultrafiltration; Membrane; Characterization; PEG; Retention

## 1. Introduction

Amongst the existing methods of separation, membranes offer many advantages such as low energy consumption or no added chemicals. In ultrafiltration, the selectivity is in part determined by the porous structure, which in turn is characterized by the sieving curves. These curves are obtained from a plot of retention of some selected solutes, called tracers, versus their molar mass.

Manufacturers generally specify for their membranes a nominal cut-off: molar mass of the solute that is (or would be) 90% retained by the membrane. However, numerous authors [1–5] have shown that the absolute membrane cut-off and the value quoted by the manufacturers may be very different because of differences in methodology and test conditions. Platt et al. [2] have investigated the difference between membrane cut-offs measured via single solute experiments and the values quoted by the manufacturers. For all membranes investigated, the measured cut-off was different from the manufacturer's one. However, a conclusion is difficult to draw here as the characterization method used by the manufacturers is not exposed, making difficult an evaluation of the origin of the difference.

If the aim is a comparative characterization of membranes, the absolute values for the cut-off are of secondary importance. However, in water treatment for example, Jacangelo et al. [3] underline that quantification of an absolute cut-off is one critical factor in assessing whether a membrane has a potential to remove such particle or microorganism. In the same way, in pharmaceutical industries where the application calls for the separation of molecules whose molar masses are not greatly dissimilar, product quality requires that the membranes have a consistent cut-off value and that any change in the cut-off of the membrane whilst in use, are capable of being monitored [4].

Recent works show that the cut-off obtained according to methods using dextrans as tracers is not modified by the creation of few defects (1000–5000 times larger than the mean pore radius) in the membrane structure [6]. This underlines the necessity to improve the characterization method and that cut-off values do not provide information on the sharpness of the selectivity based on the breadth of the pore size distribution [5,7].

* Corresponding author. Tel.: +33-5-61558690; fax: +33-5-61556139.
*E-mail address:* caussera@chimie.ups-tlse.fr (C. Causserand).

In this paper, we propose an analysis of previous works on UF membrane characterization by measurements of tracer retention, in order to underline critical points in previously reported techniques. We then suggest to adapt existing methods in order to improve both experimental conditions and data treatment. We then show two examples for which the proposed method has proved to be accurate and reproducible.

## 2. Background

### 2.1. Models for membrane retention calculation

Due to its porosity, the selectivity of a filtration membrane is partly controlled by the steric effect, which depends on the shape and size of the solute and pores. Charge effects can also be taken into consideration in the case where solutes and membrane surface are charged. This phenomenon will be considered negligible in this paper as (i) tracers used are neutral, (ii) the density of charge of the membrane being low, the energy of interaction between neutral solutes and the membrane can be assumed negligible compared to the energy of interaction due to steric hindrance. This selectivity, combined to the convective and diffusive fluxes controls the overall transfer of solute.

A complete and accurate description of solute transport (sieving) during membrane filtration requires the knowledge of two parameters: the asymptotic retention coefficient $R_{inf}$ which describes the convective contribution to the solute flux and the Peclet number in the pores $Pe_{pore}$ which describes the relative importance of solute convection to diffusion inside the membrane [8]. $R_{inf}$ defined by Eq. (1) is the only intrinsic characteristic of the membrane/solute system since it only depends on geometric dimensions pores with regards to a given solute, and is not dependent on transport phenomena:

$$R_{inf} = 1 - \phi K_c \tag{1}$$

with $\phi$ being the solute equilibrium partition coefficient between the membrane phase and the adjacent liquid phase and $K_c$ the hindrance factor for convection. The peculiarity of the asymptotic retention coefficient is that its value cannot be measured directly as it would require very high filtration fluxes, without concentration polarization (i.e. infinite mass transfer coefficient) [8].

Transport in porous membranes has been described by different approaches as summarized by Opong and Zydney [8]. In all these approaches the solute flux through the membrane is given by the sum of the convective and diffusive contributions. The results are conveniently expressed in some studies in term of an "actual sieving coefficient" $S_a$ [8] defined as the ratio of the solute concentration in the permeate ($C_p$, kg m$^{-3}$) to that at the membrane surface ($C_m$, kg m$^{-3}$) or in other works in term of "membrane retention coefficient", $R_m$ [9]:

$$R_m = 1 - S_a = 1 - \frac{C_p}{C_m} \tag{2}$$

By using this last description, the integration across the membrane of mass transfer equation allows the link between $R_{inf}$ and the membrane retention coefficient $R_m$ to be established:

$$R_m = 1 - \frac{(1 - R_{inf})\exp(Pe_{pore})}{\exp(Pe_{pore}) - R_{inf}} \tag{3}$$

where

$$Pe_{pore} = \frac{J}{k_{pore}} \tag{4}$$

and

$$k_{pore} = D_\infty \frac{\varepsilon}{L}\frac{K_d}{K_c} \tag{5}$$

with $D_\infty$ being the infinite dilution diffusion coefficient (m$^2$ s$^{-1}$), $\varepsilon$ the porosity of the membrane and $L$ the pore length (taken equal to skin thickness, m), $J$ the flux density (m$^3$ m$^{-2}$ s$^{-1}$), $k_{pore}$ the transfer coefficient in the pores (m s$^{-1}$) and $Pe_{pore}$ the Peclet number in the pores. The hindrance factors $K_c$ and $K_d$ are, respectively, the convective and diffusive correction coefficients that reflect the additional drag on the solute molecule due to the presence of the pore walls. Deen [10] has reviewed most of the experimental and theoretical works on hindered transport and gave several analytical expressions for these hindrance factors.

Considering Eq. (3), we can see that $R_{inf}$ is the asymptotic value of $R_m$ at infinite $Pe_{pore}$. Unfortunately, $R_{inf}$ and $R_m$ cannot be, in principle, determined directly by experimental measurements due to concentration polarization [8]. Nevertheless, a direct estimation of $R_m$ can be achieved in some particular operating conditions such that the effect of concentration polarization is negligible (see Section 2.2.1).

Concentration polarization is modeled by the film relationship that relates the membrane retention coefficient $R_m$ and the observed retention coefficient $R_{obs}$:

$$\ln\left(\frac{1 - R_{obs}}{R_{obs}}\right) = \ln\left(\frac{1 - R_m}{R_m}\right) + \left(\frac{J}{k_{BL}}\right) \tag{6}$$

which can be noted

$$R_{obs} = \frac{1}{1 + ((1 - R_m)/R_m)\exp(Pe_{BL})} \tag{7}$$

where

$$R_{obs} = 1 - \frac{C_p}{C_r} \tag{8}$$

$$Pe_{BL} = \frac{J}{k_{BL}} \tag{9}$$

and

$$k_{BL} = \frac{D}{\delta} \tag{10}$$

with $C_r$ being the concentration in the retentate ($kg\,m^{-3}$), $k_{BL}$ the mass transfer coefficient in the boundary layer ($m\,s^{-1}$), $Pe_{BL}$ the Peclet number in the boundary layer, $\delta$ the boundary layer thickness (m) and $D$ the average solute diffusion coefficient in the mass transfer boundary layer (often taken equal to infinite dilution diffusion coefficient $D_\infty$, $m^2\,s^{-1}$).

Eq. (6) allows $R_m$ to be determined if a straight line is obtained when plotting $\ln((1-R_{obs})/R_{obs})$ versus flux $J$ [11].

For the purpose of the determination of an asymptotic retention coefficient, the combination of Eqs. (3) and (7) provides an adequate link between $R_{obs}$ and $R_{inf}$. Eq. (11) takes into account transfer in the pore and boundary layer and selectivity:

$$R_{obs} = \frac{1}{1 + ((1 - R_{inf})\exp(Pe_{BL}))/(R_{inf}(1 - \exp(-Pe_{pore})))} \tag{11}$$

For large $Pe_{pore}$, Eq. (11) is equivalent to Eq. (7) in which $R_m$ would substitute for $R_{inf}$.

In order to illustrate previous comments, we report in Fig. 1 the theoretical general evolution of $R_{obs}$, $R_m$ and $R_{inf}$ as a function of $Pe_{pore}$ assuming that $Pe_{pore} = B\,Pe_{BL}$. $B$ is a constant characteristic of the membrane and of the filtered solute for fixed hydrodynamic conditions [12]:

$$B = \frac{Pe_{pore}}{Pe_{BL}} = \frac{k_{BL}}{k_{pore}} = \frac{L}{\varepsilon}\frac{1}{\delta}\frac{K_c}{K_d} \tag{12}$$

This parameter has been taken equal to 1 in Fig. 1. The difference between $R_{obs}$ and $R_m$ varies according to the values of $Pe_{BL}$ and $Pe_{pore}$ [12–14]. For low Peclet numbers (small solute with large diffusion or/and low convection), there is a negligible concentration polarization ($Pe_{BL} < 0.1$) but an important diffusion in the porous medium leads to a dispersion and then to a poor retention, as a consequence $R_{obs}$ and $R_m$ show the same evolution. In case of intermediate Peclet numbers, there is a low polarization and a low dispersion in the porous medium leading to large solute retention ($R_{obs}$ maximum value). At higher Peclet numbers, convection in the membrane becomes the most important phenomenon due to a negligible dispersion by diffusion in the porous medium ($Pe_{pore} > 2$) but simultaneously the concentration polarization is accentuated ($Pe_{BL} > 1$) that induces a low observed retention, $R_{obs}$ decreases towards null retention and $R_m$ always increases up to its limit, $R_{inf}$. The coordinates of the maximum in $R_{obs}$ versus $Pe_{pore}$ curve are given by the following equations [12]:

$$Pe_{pore,max} = \ln(B + 1) \tag{13}$$

$$R_{obs,max} = \frac{1}{1 + ((1 - R_{inf})/R_{inf})((1 + B)^{B+1/B}/B)} \tag{14}$$

Opong and Zydney [8] have used such considerations to explain the maximum value found when plotting retention versus filtrate flux in bovine serum albumin filtration. They calculate the value of the membrane retention coefficient at $R_{obs,max}$ and show that, even at the maximum in $R_{obs}$, $R_m$ is equal to $R_{inf}$ only if $B \gg 1$. Opong and Zydney mention that this situation is relatively easy to satisfy with most track-etched membrane since $\varepsilon$ is very small (<0.01) and $L$ is of the order of 10 μm ($\varepsilon/L \approx 1 \times 10^{+3}\,m^{-1}$). The situation is very different for asymmetric membranes due to a large porosity and the very small skin thickness ($\varepsilon/L \approx 1 \times 10^{+6}\,m^{-1}$). This constraint on $B$ is also difficult to meet in cross-flow membrane devices as it corresponds to low boundary layer thickness $\delta$. Thus, they conclude that considerable care must be taken in interpreting published results for the retention coefficients of asymmetric ultrafiltration membranes, many of which may be above $R_{inf}$ due to the effects of solute diffusion and bulk mass transport.

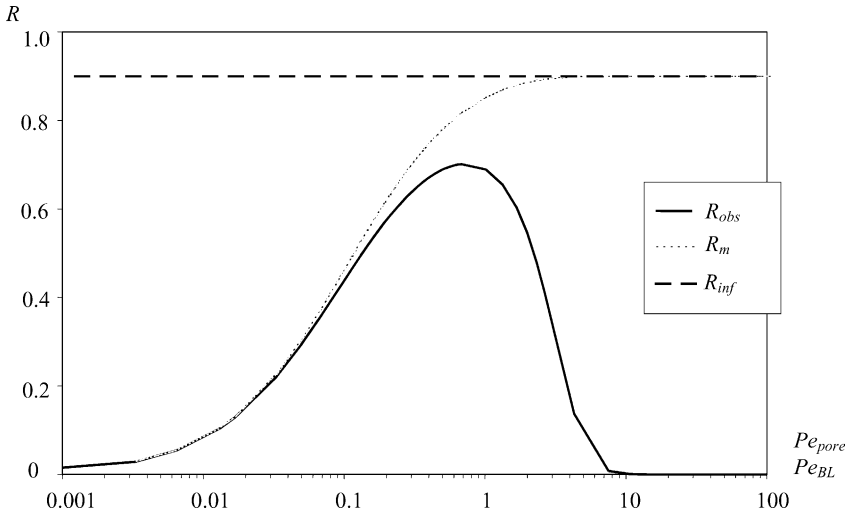


Fig. 1. Retention coefficient evolution for neutral solutes vs. $Pe_{pore}$, $Pe_{BL}$.

### 2.2. Characterization method by measurements of tracers' retention

The main characteristics of an UF membrane displayed in commercial catalogues are its permeability ($L_p$) and its cut-off (classically noticed MWCO). The cut-off, directly related to the properties of membrane retention, is deduced from the characteristic retention curve at 90% retention. This curve represents the evolution of the observed retention coefficient $R_{obs}$ as a function of the solute molar mass. Numerous works have already been published reporting investigations on the choice of tracers' solution, but also on experimental procedure and data treatment method in order to obtain sieving curve and cut-off with the maximum accuracy.

#### 2.2.1. Choice of tracers solution

The choice of tracers has to consider multiple criteria, such as: (i) well defined size; (ii) interactions with membrane as low as possible so as to reduce fouling during the characterization procedure; (iii) they must be available in a large range of sizes; (iv) reasonable price.

These are various types of tracers already used in ultrafiltration: dextrans (flexible polysaccharides [1,5–7,15]), poly(ethylene glycol)s (PEG [2,16]), polyvinylpyrollidone (PVP) and proteins (BSA, α-lactalbumin, β-lactoglobulin, etc.) [17]. In the case of polysulfone membranes (membrane material used in the present work), tracers usually used are dextrans and PEGs as they do not adsorb much on this type of membranes [18,19].

The characterization tests can be performed according the French Standard NF X 45-103 ([20], partly based on [18]). It is based on retention measurements of dextran molecules prepared in mixture and filtered at various trans-membrane pressures chosen in such a way that low concentration polarization occurs.

In general, the tracer solution to be used for the ultrafiltration experiments should be prepared with molecules covering a broad molar mass range, corresponding to retention coefficients ranging from almost 0 to 100% [18].

Some authors [1] mention that characterization experiments with mixtures of one kind of polymer with a defined composition and a wide molecular distribution like dextrans are simpler because a single run is sufficient to obtain a full $R_{obs} = f(MM)$ curve. However, this advantage has to be traded with the fact that samples analysis by gel permeation chromatography and data treatment on the chromatograms are time consuming and less accurate than an analysis by spectrophotometry (for proteins) or by total organic carbon analysis (for single sized PEG). Also, one can speculate that larger tracer molecules, which accumulate in the boundary layer, enhance the retention of smaller ones due to steric hindrance at the pore inlet [15,19]. Tam and Tremblay [19] mention that the advantage offered by the mixed solute method is then reduced due to the measured cut-off being underestimated.

According to the previous discussion, we expect that the single sized solute filtration experiments are more accurate and then more adequate than filtration of mixtures when a precise characterization is searched for.

#### 2.2.2. Experimental procedure and data treatment method

Manufacturers and a majority of membrane end-users usually follow a simplified procedure that consists in a filtration of tracers at a defined (and sometimes non published) trans-membrane pressure and concentration polarization is unavoidable. As a consequence, Schlichter et al. [1] have shown that even a minor trans-membrane pressure increase of 0.2 bar can result in the apparent cut-off being doubled. This pressure dependence emphasizes the necessity to minimize and even to cancel the effects of concentration polarization in the determination of a retention curve in order to be able to consider it as characteristic of the membrane porous structure. For this reason numerous authors have focused part of their work on defining the conditions for retention measurements in the absence or with a weak polarization effect.

Platt et al. [2] have summarized previous studies [11,15,19] on the evolution of the concentration polarization modulus $C_m/C_r$ as a function of the ratio $J/k_{BL}$. These results show the range that $J/k_{BL}$ should be within, for concentration polarization not to alter the retention. In these conditions, $R_m$ can be assumed equal to the observed retention $R_{obs}$.

Other authors [11,18] suggest that at high concentration polarization modulus, $\ln((1 - R_{obs})/R_{obs})$ is plotted versus the trans-membrane pressure for each molar mass tracer and extrapolated to zero pressure (or, what is the same thing, zero permeation flux) in order to obtain, according to the "concentration polarization model" (Eq. (6)), the membrane retention coefficient $R_m$. This allows a curve $R_m = f(MM)$ to be obtained and a cut-off determined.

An explanation for the discrepancy between characteristic retention curves obtained by various researchers on a same membrane can be the type of parameter used to refer to a tracer. Meireles et al. [21] have measured the transport of different series of solutes (PEGs, dextrans and proteins) through UF membranes of various cut-off. These authors show that when the retention coefficients are plotted as a function of molar mass, a curve is obtained for each series of solute whereas when data are plotted versus the hydrodynamic radius, retention coefficients fall close to a single retention curve for each membrane. This latter parameter then provides a good description of the actual volume occupied by a molecule traveling by convection in a pore. The hydrodynamic radius then seems to be more appropriate than the molar mass for a standard characterization of membranes, since it should allow to predict the behavior of one class of solutes from the data collected with a different class. One can then also determine, rather than a cut-off expressed in molar mass, the hydrodynamic radius of the molecule retained at 90% by the membrane (size cut-off).

## 3. Developed characterization method

According to the previous discussion, to minimize and even cancel the effects of concentration polarization in the determination of a sieving curve, two methods are available. The first method involves successive filtrations at various trans-membrane pressures (or various permeation fluxes) of the same solution in order to obtain, by extrapolation, the retention at zero pressure (or zero flux) using Eq. (6). The second one requires the choice of flux and cross-flow velocity for each tracer used so that the calculated $J/k_{BL}$ values correspond to negligible concentration polarization. In this latter case, only one experimental permeation flux has to be studied. The two methods end up to a curve $R_m = f(MM)$ which provides, in most cases, a satisfactory membrane characterization. However, as mentioned in Section 2.1 and shown in Fig. 1, $R_m$ cannot be considered as an intrinsic characteristic of the membrane. As a consequence, the cut-off deduced from the curve $R_m = f(MM)$ might be more or less "conditions" dependent, especially for small molecules and membrane of low permeability and therefore not adapted for a reliable study of membrane structure evolution.

### 3.1. Experimental procedure

Here the properties of the studied membrane being a priori unknown, a standard experimental procedure is used for its characterization: successive permeation at various fluxes of given tracers at one given concentration. In this paper, we report on works on membrane characterization that has been developed for two different projects:

- The monitoring of the integrity of a membrane during an accelerated ageing process specifically in water treatment. During normal operation in water production, membranes periodically undergo chemical cleaning. The contact with these solutions certainly plays an important role on membrane ageing and, as a result, on their lifetime; however the kinetics of this degradation and its consequences on membrane properties are still poorly understood. To study the membrane structure evolution, accelerated ageing of the membrane is looked for by soaking it in chemical solutions. Membrane properties are then monitored as a function of contact-time by means of various characterization methods including measurement of tracer' retention.
- The characterization of membranes modified by UV grafting. The development of a new composite UF membrane less sensitive to fouling during treatment of dye effluents has been investigated in our laboratory [22]. This new membrane was obtained by photo-grafting a polymer on the surface of a polysulfone ultrafiltration membrane. This grafting induces not only surface property modifications but also a decrease in cut-off from approximately 10 to around 2–5 kg mol$^{-1}$ (deduced from PEG filtration). The aim here is an accurate quantification of the cut-off change as a function of operating conditions chosen for the modification stage such as the velocity of fibers in the UV reactor.

Table 1
Main characteristics of tracer solutions used in membrane characterization

| MM (kg mol$^{-1}$) | $r_{hyd}$ (nm) | $D_\infty$ (m$^2$ s$^{-1}$) | Supplier |
|---|---|---|---|
| PEG | | | |
| 1 | 1.3 | $2.3 \times 10^{-10}$ | Aldrich |
| 2 | 1.9 | $1.7 \times 10^{-10}$ | Aldrich |
| 4.6 | 3.0 | $1.2 \times 10^{-10}$ | Aldrich |
| 10 | 4.6 | $0.8 \times 10^{-10}$ | Fluka |
| 20 | 6.7 | $0.6 \times 10^{-10}$ | Fluka |
| 35 | 9.2 | $0.5 \times 10^{-10}$ | Fluka |
| 100 | 16.4 | $0.3 \times 10^{-10}$ | Aldrich |
| Dextran T10 | | | |
| 10 | 3.6 | $0.9 \times 10^{-10}$ | Pharmacia |

These studies require a characterization method sufficiently sensitive to small structural changes of the membrane. In a second step, we have adapted the method in order to reduce the experimental workload, without, hopefully, loss of sensitivity. This part of the study specifically concerns the monitoring of the integrity of a membrane that involves numerous sample characterizations.

### 3.2. Experimental data processing

The procedure consists in adjusting parameters (retention coefficient, mass transfer coefficients) so as to minimize the sum of the squared residuals between experimental and calculated retention $R_{obs}$ in Eq. (11).

In this procedure we observed that many combinations of parameters ($k_{BL}$, $k_{pore}$) could fit Eq. (11) to experimental data. We then made the choice of using particular parameter values in the initialization stage of the method. $R_{inf}$ and $k_{BL}$ were initialized with $R_m$ and $k^*_{BL}$ values obtained by fitting Eq. (7) to experimental data. Initial $k_{pore}$ is calculated using $D_\infty$ (Table 1), $\varepsilon/L$ ratio (provided by the manufacturer) and $K_c$ and $K_d$ for each PEG. These two last parameters are calculated from analytical expressions developed for spherical solutes in cylindrical pores using the centerline approximation [10]. These expressions are valid for all values of the ratio of the solute ($r_{hyd}$) to pore ($r_{pore}$) radii ($\lambda$). Tracer hydrodynamic radius $r_{hyd}$ is calculated as a function of solute molar mass (see Section 4.1). A pore radius $r_{pore}$ is estimated for each molar mass tracer by using Ferry's equation and $R_m$. This procedure reduces the degree of freedom of the method and leads to consistent $k_{pore}$ values (Eq. (5)). Tests have been conducted in order to evaluate the sensitivity of $R_{inf}$ best fit value to $k_{pore}$ initialization. Various values, corresponding to calculated $k_{pore} \pm 20\%$, have been used in initialization stage and we obtained the same $R_{inf}$.

We can then compare two retention curves: $R_m$ (Eq. (7)) and $R_{inf}$ (Eq. (11)) versus tracer hydrodynamic radius, and consequently determine in each case a cut-off.

The experimental part includes the filtration of:

- six single sized PEGs at 6 values of flux each for UF membrane (i.e. 36 experiments per characterization);
- three single sized PEGs at 5 values of flux each for UF-grafted membrane (i.e. 15 experiments per characterization).

For the purpose of monitoring the changes in the characteristic retention curve of the UF membrane during its accelerated ageing process, the previous method has to be periodically repeated, sometimes everyday. For this, it is necessary to reduce the experimental workload as much as possible. The idea here is to consider that during the ageing process the mass transfer coefficient $k_{pore}$ for a same tracer remains in the same range of value. Moreover, the same filtration module and hydrodynamic conditions are used so as $k_{BL}$ also remains constant.

The full procedure previously presented is then only applied to the virgin membrane to determine $k_{BL}$ and $k_{pore}$ that are assumed constant throughout further experiments, which allows simplification of the procedure, as described below.

From the $R_{obs}$ versus $J$ curves obtained for each PEG, we select a tracer (of size around the virgin membrane cut-off) and a filtration flux $J^*$ that is a value within the range of the $R_{obs}$ versus $J$ curves for the selected tracers. If more than one tracer were chosen, it may happen that no $J^*$ flux value common to all the curves is found. This is often due to the low flux values obtained during filtration of the higher molar mass tracers that are dissolved at the same concentration as the smaller ones. The tracer concentration has then to be adjusted. Otherwise, the experimental part in the simplified procedure is reduced to one experiment.

Thanks to the knowledge of $k_{BL}$ and $k_{pore}$ deduced from the full procedure on the virgin membrane and the fixed flux $J^*$, constant parameters appear in Eq. (11) that can be written as follows:

$$R_{inf} = \frac{A_1 R_{obs}}{A_1 R_{obs} - A_2(R_{obs} - 1)} \tag{15}$$

with

$$A_1 = \exp\left(\frac{J^*}{k_{BL}}\right) \tag{16}$$

and

$$A_2 = 1 - \exp\left(\frac{-J^*}{k_{pore}}\right) \tag{17}$$

From Eq. (15) we can then deduce the asymptotic retention coefficient $R_{inf}$ from the experimental measurement of $R_{obs}$.

Changes in $R_{obs}$ and hence in $R_{inf}$ of this molecule can be monitored during the membrane modification (ageing, grafting, etc.).

## 4. Materials and experimental set-up

### 4.1. Solutes and analytical equipment

A characteristic retention curve has been obtained by filtration of solutions at $1\,g\,L^{-1}$ of monodispersed PEGs. This relatively small concentration ensures minimal solute–solute interactions. PEGs used for the characterization of UF membranes range from 2 to $100\,kg\,mol^{-1}$. In the case of UF-grafted membranes PEGs 1, 4.6 and $10\,kg\,mol^{-1}$ have been used. All the solutions were prepared from RO-treated water.

PEG samples were analyzed by a total organic carbon analyzer (TOC-5050A, Shimadzu, Japan).

The filtration of a solution $0.5\,g\,L^{-1}$ of polydispersed dextran T10 has also been conducted in order to compare the retention obtained with the two types of solutes. Sodium azide (Aldrich) was added at a concentration of $0.1\,g\,L^{-1}$ in dextran T10 to prevent bacterial growth, as these samples have been stored in the fridge before analysis.

Feed and permeate dextran samples were analyzed by gel permeation chromatography (GPC) using a TSK G4000 SW column coupled with a Waters refractive index detector.

The main characteristics of the tracer solutions filtered are summarized in Table 1.

In the case of PEGs, the hydrodynamic radius is calculated by Eq. (18) [21]:

$$r_{hyd} = \left(\frac{3[\eta]MM_{PEG}}{4\pi\xi N}\right)^{1/3} \tag{18}$$

where

$$[\eta] = 4.9 \times 10^{-8}(MM_{PEG})^{0.672} \tag{19}$$

with $[\eta]$ being the intrinsic viscosity of the solution ($m^3\,g^{-1}$), $[\eta]MM_{PEG}$ the hydrodynamic volume ($m^3\,mol^{-1}$), $\xi$ the constant proportionality between the radius of the equivalent sphere and the radius of gyration of the polymer molecule (taken as equal to 1) and $N$ the Avogadro number ($mol^{-1}$).

### 4.2. Membranes

Hollow fibers UF membranes (inner skinned, $D_i = 9.6 \times 10^{-4}$ m) have been supplied by Aquasource (Toulouse, France). They are made of polysulfone modified by surface grafting of hydrophilic groups. Nominal cut-off and estimated $\varepsilon/L$ provided by the supplier are $40\,kg\,mol^{-1}$ and $1 \times 10^{+5}\,m^{-1}$, respectively.

UF-grafted membranes were manufactured in the laboratory by UV-photopolymerization of sodium *p*-styrene sulfonate monomer on the surface of a polysulfone ultrafiltration hollow fiber with external skin [22] ($D_e = 1.2 \times 10^{-3}$ m). The estimated cut-off is around $10\,kg\,mol^{-1}$ before modification and between 2 and $5\,kg\,mol^{-1}$ after grafting. The ratio $\varepsilon/L$ is estimated around $5 \times 10^{+4}\,m^{-1}$ from data provided by the manufacturer (Akbari et al.).

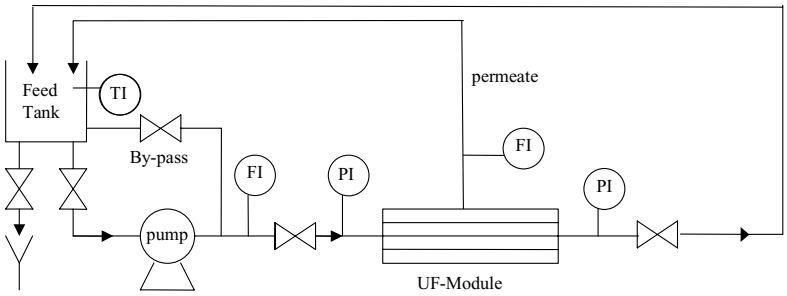


Fig. 2. Experimental set-up.

### 4.3. Filtration set-up and procedure

Tracer solutions have been filtered on a cross-flow filtration bench with hollow fiber modules (Fig. 2). Each module tested contains 16 fibers in the case of UF membranes (area $\sim 1.5 \times 10^{-2}\,m^2$) and 6 fibers in the case of UF-grafted membranes (area $\sim 4.8 \times 10^{-3}\,m^2$). The hydrodynamic conditions correspond to laminar flow ($Re_{UF} = 1800$, $Re_{UF\text{-grafted}} = 1280$). The desired pressure, adjusted by means of valve, was varied in the range of 0.3–0.8 bar for UF membrane and 0.5–3 bars for UF-grafted membrane, giving fluxes in the range of 12–66 and 4–29 $\mu m\,s^{-1}$, respectively. The permeate was recycled to maintain a constant volume (and concentration) in the tank. Once the flux had stabilized (after a filtration period of 20 min), 10 mL filtrate and retentate samples were collected for subsequent analyzis.

Experiments with UF-membrane were performed at the temperature $15 \pm 2\,^{\circ}C$, which is measured in the tank at the beginning and end of the filtration. The evolution of this parameter has been taken into account by correcting solution viscosity (taken as equal to water viscosity) and then permeation flux value by the use of empirical relationship derived from water viscosity measurements at different temperatures [23]. For experiments with UF-grafted membrane, the tank temperature was maintained at $20\,^{\circ}C$.

The membrane water permeability was measured before each experiment. The UF membrane permeability is $10^{-12}\,m \pm 4\%$ and the permeability after grafting is approximately $10^{-14}\,m \pm 3\%$.

After filtration of a tracer solution, the rig is flushed with 10 L of RO-treated water and membrane permeability is again determined. The loss of permeability was <5%, which is in agreement with AFNOR standard [20].

## 5. Experimental results and discussions

### 5.1. UF membrane

Fig. 3 shows the observed retention of various PEGs and one dextran versus filtration flux for the virgin UF membrane. We observe that in the same conditions of flux, $R_{obs}$ are higher for the PEG than for dextran of same nominal molar mass. Kim et al. [5] observed the same behavior and report that the difference can be attributed to differences in the molar mass distribution of the two solutes: as already mentioned PEGs are monodispersed tracers compared to dextrans that always show a more or less wide molar mass distribution. They also suggest that the differences in interactions between the solute and the membrane can play a role, even if these interactions are weak. However for

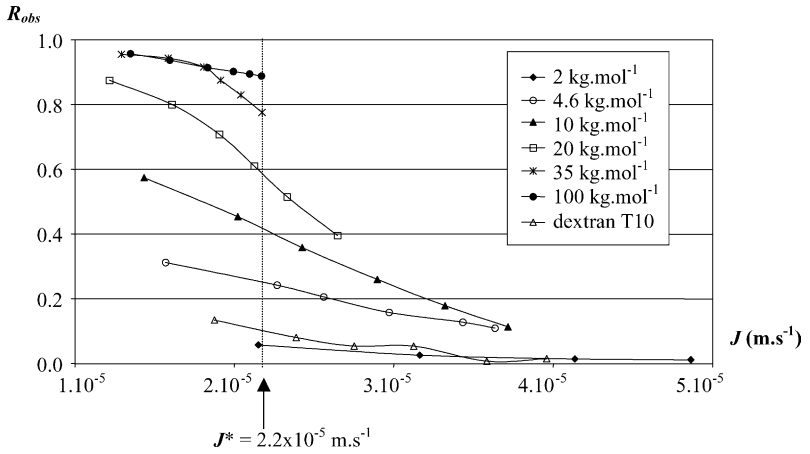


Fig. 3. Experimental $R_{obs}$ vs. permeation flux for various PEGs and one dextran (T10) filtered on UF membrane.

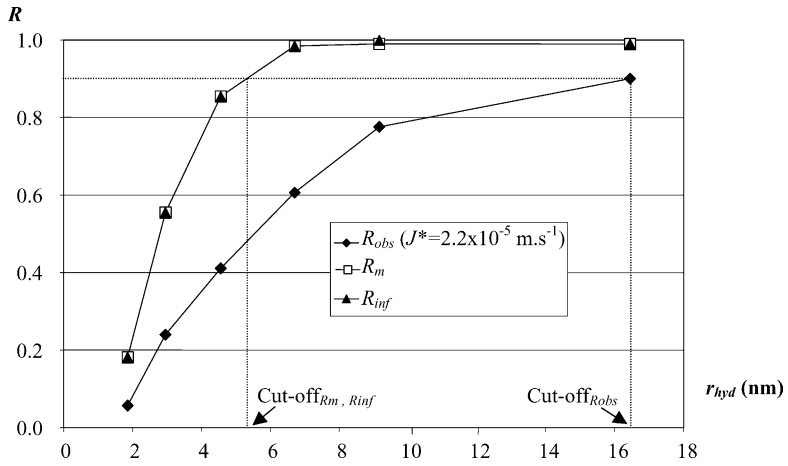


Fig. 4. Characteristic retention curve of virgin UF membrane used to determine cut-off. Comparison between the curves obtained from the plot of $R_{obs}$ ($J^* = 2.2 \times 10^{-5}\,m\,s^{-1}$), $R_m$ (Eq. (7)) and $R_{inf}$ (Eq. (11)).

a same molar mass PEG has a larger hydrodynamic radius than dextran (Table 1), and this is probably the main explanation of such a difference.

For all PEGs, Fig. 3 exhibits a more or less rapid decrease in retention as flux increases: our operating conditions correspond to situations where concentration polarization influences the solute transfer. This will be confirmed later in the discussion by the calculation of $Pe_{BL}$ range corresponding to flux (12–66 $\mu m\,s^{-1}$) and molar mass (2–100 $kg\,mol^{-1}$) ranges used in the characterization procedure.

Treatment of data reported in Fig. 3 allows the determination of coefficients $R_{inf}$ and $R_m$ that are reported versus tracer hydrodynamic radius in Fig. 4. We observe that whatever the size of the PEG filtered, $R_m$ and $R_{inf}$ are similar.

Mass transfer coefficients (Eqs. (7) and (11)), $B$ and Peclet numbers, obtained from data reported in Fig. 3, are summarized in Table 2. The first remark is that whatever the model used, $k_{BL}$ coefficients decrease with increasing molar mass, which is consistent with a decrease in diffusion coefficient with increasing molar mass [11,24]. The second observation is that $k_{BL}$ best fit values obtained from the two models are identical. This observation confirms the results shown in Fig. 4: concentration polarization model (Eq. (7)) provides satisfactory evaluation of intrinsic retention of the membrane and solute transfer in the boundary layer whatever the hydrodynamic radius of the PEG filtered (in the range of 1.3–16.4 nm; corresponding to molar masses from 2 to 100 $kg\,mol^{-1}$). The range of $Pe_{BL}$ thus obtained ($0.98 < Pe_{BL} < 5.69$) confirms a significant concentration polarization as flux increases.

As for $k_{BL}$ evolution, $k_{pore}$ decreases with increasing molar mass that is consistent with a decrease in $D_\infty$ and $K_d/K_c$ ratio as tracer molar mass and hence solute radius increase. Furthermore, $k_{pore}$ is from 10 to 3400 fold lower than $k_{BL}$: diffusion in the pore is low as compared to that in the boundary layer transfer (see Table 2).

In Fig. 4 we also report $R_{obs}$ values obtained at fixed flux $J^*$ of $2.2 \times 10^{-5}\,m\,s^{-1}$ in order to illustrate the overestimation of cut-off when the observed retention is used directly. The hydrodynamic radius of the PEG retained at 90% is 5.3 nm when deduced from $R_{inf}$ or $R_m$ and 16.4 nm from $R_{obs}$. The range of $Pe_{BL}$ corresponding to our operating conditions with a fixed flux of $2.2 \times 10^{-5}\,m\,s^{-1}$ is higher than the one recommended by Platt et al. [2]. These authors report that $Pe_{BL}$ should be in the range of 0.405–0.693 for $R_m$ to be considered as equal to $R_{obs}$.

In Fig. 5, we show the evolution of calculated $R_{obs}$ all over the range of $Pe_{pore}$ by using Eqs. (7) and (11) and six

Table 2
Mass transfer coefficient of PEGs in the boundary layer and pore for a virgin UF membrane

| | $MM_{PEG}$ ($kg\,mol^{-1}$) | | | | | | | | | | | |
|---|---|---|---|---|---|---|---|---|---|---|---|---|
| | 2 | | 4.6 | | 10 | | 20 | | 35 | | 100 | |
| $k^*_{BL}$ ($\times 10^{+6}\,m\,s^{-1}$, Eq. (7)) | 16.1 | | 16.0 | | 10.1 | | 5.77 | | 3.82 | | 8.63 | |
| $k_{BL}$ ($\times 10^{+6}\,m\,s^{-1}$, Eq. (11)) | 16.1 | | 16.0 | | 10.1 | | 5.77 | | 3.82 | | 8.63 | |
| $k_{pore}$ ($m\,s^{-1}$, Eq. (11)) | $1.80 \times 10^{-6}$ | | $1.13 \times 10^{-6}$ | | $2.03 \times 10^{-7}$ | | $8.66 \times 10^{-9}$ | | $3.87 \times 10^{-9}$ | | $2.55 \times 10^{-9}$ | |
| $B$ | 9 | | 14 | | 50 | | 666 | | 989 | | 3383 | |
| $J$ ($\times 10^{+5}\,m\,s^{-1}$) | 2.15 | 6.57 | 1.57 | 3.63 | 1.43 | 3.72 | 1.22 | 2.65 | 1.29 | 2.17 | 1.35 | 2.17 |
| $Pe_{BL}$ | 1.34 | 4.09 | 0.98 | 2.27 | 1.41 | 3.66 | 2.11 | 4.59 | 3.38 | 5.69 | 1.56 | 2.51 |
| $Pe_{pore}$ | 11.9 | 36.5 | 13.9 | 32.2 | 70.8 | 184 | 1407 | 3056 | 3340 | 5622 | 5283 | 8503 |

Peclet number ranges used in the characterization procedure and $B$ parameter values,

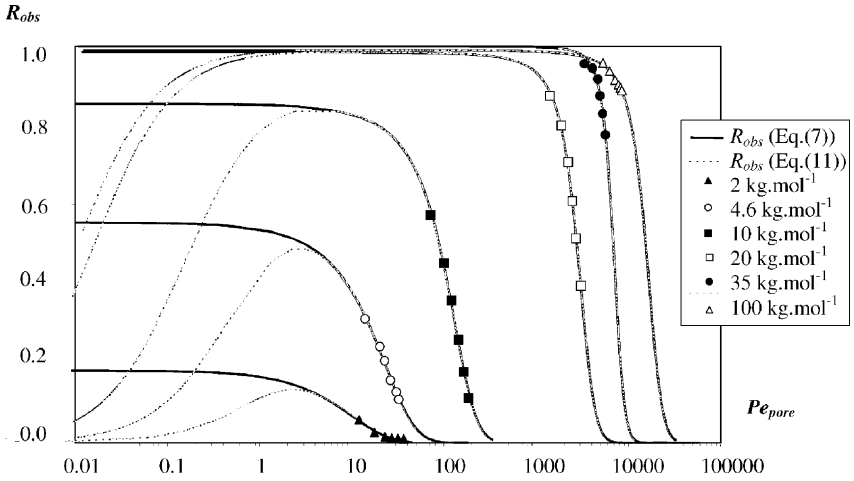


Fig. 5. Calculated $R_{obs}$ vs. $Pe_{pore}$ for the UF membrane, by using concentration polarization model (Eq. (7)) or developed method (Eq. (11)).

series of experimental data (symbols) using the parameters corresponding to PEGs 2, 4.6, 10, 20, 35 and 100 kg mol$^{-1}$. The solid and dashed curves represent the calculated values of $R_{obs}$ by using concentration polarization model (Eq. (7)) and full model (Eq. (11)), respectively.

We first observe that experimental results correspond to high Peclet number values ($Pe_{pore} = 10$). In this range of $Pe_{pore}$, Eqs. (7) and (11) provide similar data and in these conditions solute transfer is controlled by polarization concentration.

Fig. 5 also shows that increasing the solute size, that is increasing $\lambda$ (from 0.24 for PEG 2 kg mol$^{-1}$ to 0.93 for PEG 100 kg mol$^{-1}$), causes the maximum in $R_{obs}$ to shift to a higher $Pe_{pore}$ (Eq. (13)). The more rapid decrease in $K_d$ compared to $K_c$ with increasing $\lambda$ induces an increase in the ratio $K_c/K_d$ and, as a consequence, an increase in $B$ (Eq. (12)) from 9 to 3383. This induces a shift from $Pe_{pore,max} = 2.3$ for PEG 2 kg mol$^{-1}$ to 8.1 for PEG 100 kg mol$^{-1}$.

The maximum value of $R_{obs}$ increases as expected with increasing $\lambda$. However we observe in Fig. 5 that $R_{obs,max}$ is smaller than $R_{inf}$ at $\lambda$=0.24 whereas it approaches $R_{inf}$ as $\lambda \to 1$, which is confirmed by the calculation of $R_{obs,max}$ (Eq. (14)):

$$R_{obs,max}\ (\lambda = 0.24) = 0.13 \text{ to be compared to } R_{inf} = 0.18$$

$$R_{obs,max}\ (\lambda = 0.93) = 0.99 \text{ to be compared to } R_{inf} = 0.99$$

Thus, it would be possible to experimentally determine $R_{inf}$ in the case of high molar mass tracer (20–100 kg mol$^{-1}$) in conditions corresponding to $Pe_{pore}$ values around $Pe_{pore,max}$. This would require the use of filtration flux so low ($5.6 \times 10^{-8}$ m s$^{-1}$ for PEG 20 kg mol$^{-1}$, $2.0 \times 10^{-8}$ m s$^{-1}$ for PEG 100 kg mol$^{-1}$) that they cannot be considered in our characterization procedure.

As already mentioned, Opong and Zydney [8] calculate the value of the membrane retention coefficient at $R_{obs,max}$ and show that, even at the maximum in $R_{obs}$, $R_m$ is equal to $R_{inf}$ only if $B \gg 1$. In our operating conditions, this constraint on $B$ is always satisfied as $B$ is larger than 8.9 in all the cases. This is probably due to a smaller porosity of the hollow fibers studied ($\varepsilon/L \approx 1 \times 10^{+5}$ m$^{-1}$) compared to the one of asymmetric membranes mentioned by Opong and Zydney.

The difference between $R_{obs}$ values calculated by using the two models (Eqs. (7) and (11)) is reported in Fig. 6 versus $Pe_{BL}$ for various PEGs. The curves obtained confirm that whatever solute size for $Pe_{BL} = 1$ (that is always the case in the experimental part) the difference between the models is lower than 0.01%. For $Pe_{BL} < 1$ the difference rapidly increases as $Pe_{BL}$ decreases. When increasing the tracer size at constant $Pe_{BL}$, not only $D_\infty$ decreases but also $K_d/K_c$ due to the more rapid decline of $K_d$ than $K_c$ with increasing solute radius [10]. This induces an increase in $B$ and then in $Pe_{pore}$. As a consequence, Eq. (7) provides a more accurate estimation of $R_{inf}$ in the cases of high molar mass tracers (see Section 2.1). This figure allows the choice of the model used in data treatment as a function of operating conditions and error range the user decides to work in.

In the objective of monitoring the evolution of retention properties of the membrane during its accelerated ageing process, the simplified procedure developed in Section 3 has been applied.

Regarding the curves reported in Figs. 3 and 4, a unique PEG (10 kg mol$^{-1}$) has been selected ($r_{hyd} = 3.0$ nm) and filtered at constant filtration flux $J^*$ of $2.2 \times 10^{-5}$ m s$^{-1}$ on samples of membranes taken every other day.

The virgin membrane is first characterized using the full method and $R_{inf}$ (named $R_{inf,f}$), $k_{BL}$ and $k_{pore}$ are obtained. $R_{obs}$ is then determined on aged samples $R_{inf}$ (named $R_{inf,s}$) is calculated by Eq. (15) and $k_{BL}$ and $k_{pore}$ previously determined. The values deduced from the two procedures are very close to each other: $R_{inf,f} = 0.85$ and $R_{inf,s} = 0.86$.

The simplified procedure has then been used to monitor the evolution of the retention properties of the membrane during its accelerated ageing process. In the example shown here the membrane has been soaked in a solution of sodium

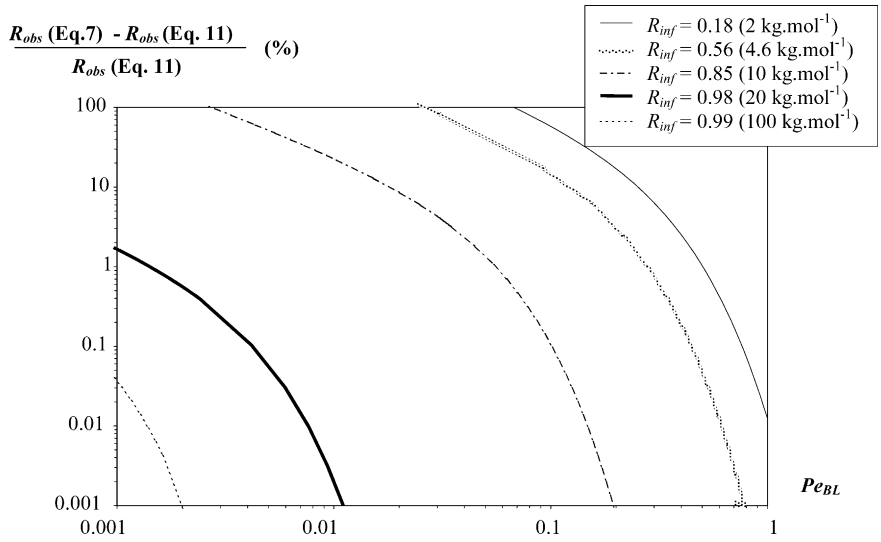


Fig. 6. Difference between $R_{obs}$ values calculated by using the two models (Eqs. (7) and (11)) vs. $Pe_{BL}$ for UF membrane.

hypochlorite 400 ppm at pH 8. The virgin membrane has been characterized by the full procedure. After 4 and 18 days in the solution of NaHClO, the membrane has been again characterized by using the simplified method. The results reported below show a decrease in PEG 10 kg mol$^{-1}$ retention which suggests a significant loss in membrane selectivity efficiency: $R_{inf,s}$ (0 day) = 0.86; $R_{inf,s}$ (4 days) = 0.82; $R_{inf,s}$ (18 days) = 0.79.

### 5.2. UF-grafted membrane

The first UF-grafted membrane characterized has been measured by the use of a linear speed $u = 4\,\mathrm{m\,min^{-1}}$ of the hollow fiber in the photo-reactor. In Fig. 7 we report observed retention coefficients for three PEGs versus filtration flux. As expected, the filtration fluxes are slightly smaller than the ones measured with the UF membrane (see Fig. 3) as the grafting process reduces the apparent pore size and/or pore density (pores/m$^2$).

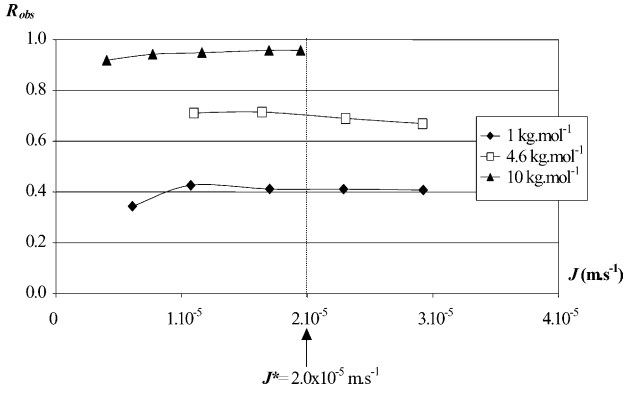


Fig. 7. Experimental $R_{obs}$ vs. permeation flux for various PEGs filtered on UF-grafted membrane.

We observe that whatever the tracer molar mass, $R_{obs}$ coefficients obtained correspond to retention around the maximum. This behavior is characteristic of situations where concentration polarization still influences the solute transfer with, in the same time, a non negligible contribution of transfer in the pore.

In a first step the fitting procedure has been applied to experimental data reported in Fig. 7 in order to determine $R_m$ and $k^*_{BL}$ by using the concentration polarization model (Eq. (7)). In a second step, by using the full model (Eq. (11)), we obtain values of $R_{inf}$, $k_{BL}$ and $k_{pore}$ for each PEG used in the characterization. As in Section 5.1, results obtained are compared.

Best fit values of $R_m$ and $R_{inf}$ are reported versus tracer radius in Fig. 8. The other parameters deduced from data treatment are summarized in Table 3. As for UF membrane we also report in Fig. 8, $R_{obs}$ obtained at fixed flux $J^*$ of $2.0 \times 10^{-5}\,\mathrm{m\,s^{-1}}$. The comparison between $R_m$ and $R_{inf}$ show a difference of 12% for PEG 1 kg mol$^{-1}$ when for higher molar mass PEGs $R_m$ and $R_{inf}$ are similar. Moreover we observe only a slight difference between $R_m$ and $R_{obs}$ ($J^* = 2.0 \times 10^{-5}\,\mathrm{m\,s^{-1}}$). If we calculate $Pe_{BL}$ range corresponding to our operating conditions (Table 3) with a fixed flux of $2.0 \times 10^{-5}\,\mathrm{m\,s^{-1}}$, we obtain $Pe_{BL} < 0.3$ (except for PEG 10 kg mol$^{-1}$). According to works reported by Platt et al. [2], these conditions correspond to a low concentration polarization modulus $C_m/C_r$, and this explains that $R_{obs}$ at $J^* = 2.0 \times 10^{-5}\,\mathrm{m\,s^{-1}}$ is only slightly smaller than $R_m$.

As a consequence of previous observations, the hydrodynamic radius of the PEG retained at 90% is 3.9 nm when deduced from $R_{inf}$ or $R_m$ and 4.2 nm from $R_{obs}$.

If we now consider the best fit values of mass transfer coefficients, we can notice a discrepancy between $k_{BL}$ obtained with the two models (Eqs. (7) and (11)) for low molar mass tracer (PEG 1 kg mol$^{-1}$). This shows that taking into account only boundary layer effect in the description of so-

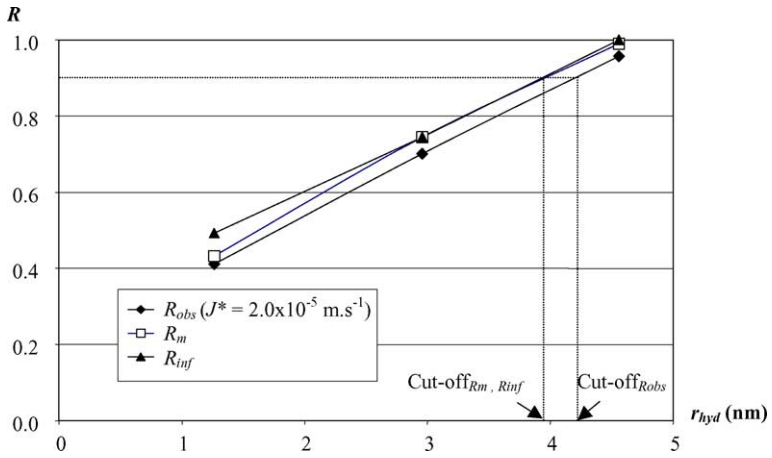


Fig. 8. Characteristic retention curve of UF-grafted membrane used to determine cut-off. Comparison between the curves obtained from the plot of $R_{obs}$ ($J^* = 2.0 \times 10^{-5}\,m\,s^{-1}$), $R_m$ (Eq. (7)) and $R_{inf}$ (Eq. (11)).

lute transfer is not sufficient in the case of low molar mass tracer. Moreover, as already mentioned in Section 5.1, we observe:

- a decrease in $k_{BL}$ with increasing molar mass (except for PEG 10 kg mol$^{-1}$ for which no satisfactory convergence has been obtained from Eqs. (7) and (11));
- a decrease in $k_{pore}$ with increasing molar mass.

The $Pe_{BL}$ corresponding to fluxes and molar masses used in the characterization procedure leads to $Pe_{BL} < 0.36$ (except for PEG 10 kg mol$^{-1}$, see Table 3). The consequence is experimental $R_{obs}$ coefficients corresponding to retention around the maximum (Fig. 7). This is verified even if the mass transfer coefficients in the pore are much lower than the ones in the boundary layer: $k_{pore}$ values are from 13-fold (for PEG 1 kg mol$^{-1}$) to 262-fold (for PEG 4.6 kg mol$^{-1}$) lower than $k_{BL}$ ones.

As previously done for the UF membrane, these experimental observations can be compared to simulation (Fig. 9) (same assumptions as in Section 5.1). Three series of data are reported using the parameters corresponding to the PEGs used: 1, 4.6 and 10 kg mol$^{-1}$. The solid and dashed curves represent the calculated values of $R_{obs}$ by using either Eq. (7) or Eq. (11). Symbols represent the experimental observed retention versus $Pe_{pore}$.

Trends are similar to those described in Fig. 5. Moreover, if we compare hydrodynamic parameters of a same PEG (i.e. 4.6 kg mol$^{-1}$) calculated for UF and UF-grafted membranes, we observe in this last case an important decrease in $K_d$ although $K_c$ is almost constant. As a consequence for UF-grafted membrane the decrease in $\varepsilon/L$ goes with an increase in $K_c/K_d$ that induces a $B$ increase far beyond 1. In these conditions, $R_{obs}$ at the maximum (and $R_m$ [8]) approaches $R_{inf}$. Previous comments are validated by the calculation $Pe_{pore,max}$ (Eq. (13)) and $R_{obs,max}$ (Eq. (14)) for PEG 1 kg mol$^{-1}$ ($\lambda$=0.41) and PEG 4.6 kg mol$^{-1}$ ($\lambda$=0.63):

$$Pe_{pore,max}\ (\lambda = 0.41) = 2.6$$

$$Pe_{pore,max}\ (\lambda = 0.63) = 5.6$$

$$R_{obs,max}\ (\lambda = 0.41) = 0.42 \text{ to be compared to } R_{inf} = 0.49$$

$$R_{obs,max}\ (\lambda = 0.63) = 0.74 \text{ to be compared to } R_{inf} = 0.75$$

Finally, whatever the tracer size, Fig. 9 confirms that operating conditions used lead to experimental $R_{obs}$ values near

Table 3
Mass transfer coefficient of PEGs in the boundary layer and in the pore for an UF membrane modified by UV-grafting at linear speed $u = 4\,m\,min^{-1}$ of the hollow fiber in the photo-reactor

| | $MM_{PEG}$ (kg mol$^{-1}$) | | | | | |
|---|---|---|---|---|---|---|
| | 1 | | 4.6 | | 10 | |
| $k^*_{BL}$ ($\times 10^{+5}$ m s$^{-1}$, Eq. (7)) | 26.3 | | 8.31 | | 91.8 | |
| $k_{BL}$ ($\times 10^{+5}$ m s$^{-1}$, Eq. (11)) | 8.26 | | 8.01 | | 0.24 | |
| $k_{pore}$ (m s$^{-1}$, Eq. (11)) | $6.58 \times 10^{-6}$ | | $3.06 \times 10^{-7}$ | | $2.42 \times 10^{-8}$ | |
| $B$ | 12.6 | | 262 | | 98 | |
| $J$ ($\times 10^{+5}$ m s$^{-1}$) | 0.61 | 2.92 | 1.10 | 2.92 | 0.40 | 1.95 |
| $Pe_{BL}$ | 0.07 | 0.35 | 0.14 | 0.36 | 1.69 | 8.19 |
| $Pe_{pore}$ | 0.92 | 4.44 | 35.9 | 95.4 | 166 | 805 |

Peclet number ranges used in the characterization procedure and $B$ parameter values.

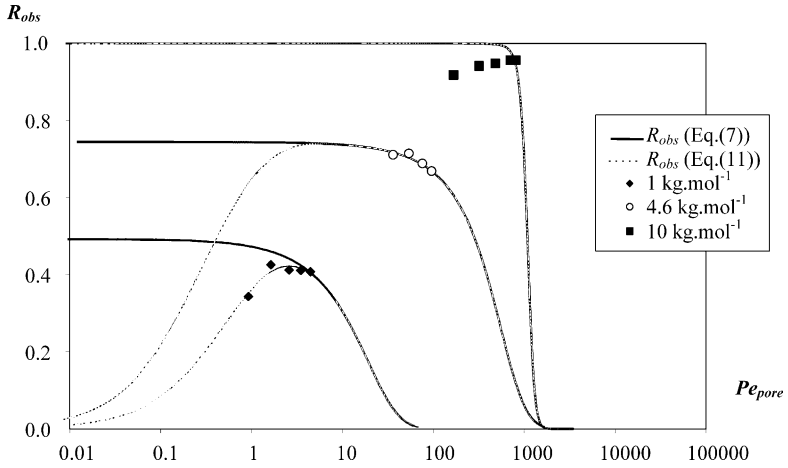


Fig. 9. Calculated $R_{obs}$ vs. $Pe_{pore}$ for the UF-grafted membrane, by using concentration polarization model (Eq. (7)) or developed method (Eq. (11)).

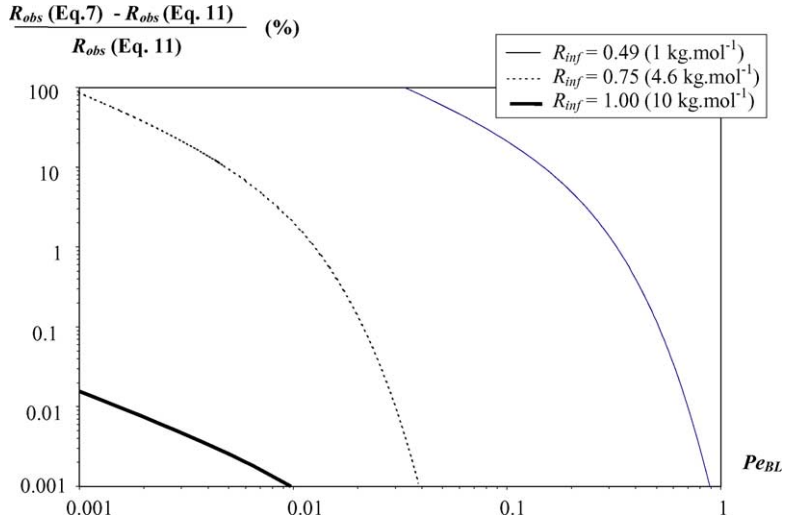


Fig. 10. Difference between $R_{obs}$ values calculated by using the two models (Eqs. (7) and (11)) vs. $Pe_{BL}$ for UF-grafted membrane.

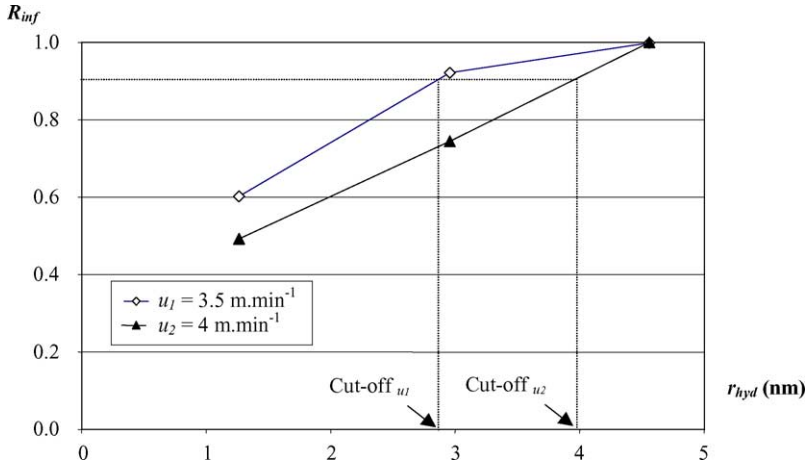


Fig. 11. Evolution of characteristic retention curve of UF membrane as a function of linear speed of the fiber in the photo-reactor during UV-grafting.

the maximum retention that approaches $R_{inf}$ as previously mentioned.

The difference between $R_{obs}$ values calculated by using the two models (Eqs. (7) and (11)) has been reported in Fig. 10 versus $Pe_{BL}$ for each molar mass PEGs. The curves obtained confirm that for $Pe_{BL} > 0.04$ and high tracer molar mass (that is the case in experimental part for PEGs 4.6 and 10 kg mol$^{-1}$) the difference between the models is lower than 0.001%. For $0.04 < Pe_{BL} < 1$ and low tracer molar mass, the difference rapidly increases as $Pe_{BL}$ decreases corresponding to experiments with PEG 1 kg mol$^{-1}$.

In order to illustrate the use of the developed method to quantify cut-off change as a function of operating conditions chosen for the UV-grafting stage, two selectivity curves are compared in Fig. 11. These curves correspond to two different grafting conditions (linear velocity $u$ of the hollow fiber in the photo-reactor). We observe an increase in cut-off from 2.6 to 3.9 nm as $u$ only increases from 3.5 to 4 m min$^{-1}$. This result is consistent with a decrease in level of grafting with the fiber residence time in the photo-reactor. This second example illustrates that the developed characterization method is sensitive to small structural changes in the membrane structure.

## 6. Conclusion

In this work, the characterization tests are performed with single sized PEGs that are filtered at various values of flux for a given molecular weight. We expect that the single sized solute filtration experiments are more accurate than filtration mixtures.

The various data treatments investigated show that in a first approximation, the concentration polarization model provides accurate results in terms of transfer and retention coefficients whatever tracer size except for low PEG molar mass filtered on UF-grafted membrane. On the other hand the curves for $R_{obs}$ fitted to the full model (Eq. (11)) are in good agreement with the experimental data over the entire range of filtrate flux ($Pe_{pore}$) whatever tracer size. In that case, the fitting procedure should be initialized using data obtained from the concentration polarization model. This provides accurate intrinsic characteristics for the membrane selectivity.

In the conditions used in the paper, the characterization method used has proved to be accurate and reproducible whatever the value of $Pe_{BL}$ used in experimental measurements and the method thus allows one to account for solute diffusion in pores, when necessary.

Finally, provided that a virgin membrane has been thoroughly characterized, the so-called "simplified" procedure allows us to characterize the membrane changes in a simplified, but accurate way. This procedure consists of a quick filtration, at one flux, with reduced number of monodispersed PEGs.


## Acknowledgements

The authors are grateful to Patrice Bacchin for helpful comments and discussions on this paper.


## Nomenclature

| | |
|---|---|
| $B$ | constant characteristic of the studied membrane and the filtered solute for fixed hydrodynamic conditions: $Pe_{pore} = B\,Pe_{BL}$ |
| $C_m$ | solute concentration at the membrane surface (kg m$^{-3}$) |
| $C_p$ | solute concentration in the permeate (kg m$^{-3}$) |
| $C_r$ | solute concentration in the retentate (kg m$^{-3}$) |
| $D$ | average solute diffusion coefficient in the boundary layer (m$^2$ s$^{-1}$) |
| $D_e$ | external diameter of hollow fibers UF membranes (m) |
| $D_i$ | inner diameter of hollow fibers UF-grafted membranes (m) |
| $D_\infty$ | infinite dilution diffusion coefficient (m$^2$ s$^{-1}$) |
| $J$ | permeation flux density (m$^3$ m$^{-2}$ s$^{-1}$) |
| $k_{BL}$ | mass transfer coefficient in the boundary layer (m s$^{-1}$) |
| $k_{pore}$ | mass transfer coefficient in the pores (m s$^{-1}$) |
| $K_c$ | hindrance factor for convection |
| $K_d$ | hindrance factor for diffusion |
| $L$ | pore length (m) |
| MM | molar mass (kg mol$^{-1}$) |
| $N$ | Avogadro number (mol$^{-1}$) |
| $Pe_{BL}$ | Peclet number in the boundary layer |
| $Pe_{pore}$ | Peclet number in the pores |
| $Pe_{pore,max}$ | $Pe_{pore}$ at the maximum in $R_{obs}$ versus $Pe_{pore}$ curve |
| $r_{hyd}$ | solute hydrodynamic radius (m) |
| $r_{pore}$ | pore radius (m) |
| $R_{inf}$ | asymptotic retention coefficient |
| $R_m$ | membrane retention coefficient |
| $R_{obs}$ | observed retention coefficient |
| $R_{obs,max}$ | observed retention coefficient at the maximum in $R_{obs}$ versus $Pe_{pore}$ curve |
| $S_a$ | actual sieving coefficient |

*Greek symbols*

| | |
|---|---|
| $\delta$ | boundary layer thickness (m) |
| $\varepsilon$ | porosity of the membrane |
| $[\eta]$ | intrinsic viscosity of the solution (m$^3$ g$^{-1}$) |
| $[\eta]$MM | hydrodynamic volume (m$^3$ mol$^{-1}$) |
| $\lambda$ | ratio of solute radius to pore radius |

| | |
|---|---|
| $\xi$ | constant proportionality between the radius of the equivalent sphere and the radius of gyration of the polymer molecule |
| $\phi$ | solute equilibrium partition coefficient |

## References


[1] B. Schlichter, V. Mavrov, H. Chmiel, Comparative characterization of different commercial UF membranes for drinking water production, J. Water Supply: Res. Technol.-AQUA 49.6 (2000) 321–328.

[2] S. Platt, M. Mauramo, S. Butylina, M. Nyström, Retention of pegs in cross-flow ultrafiltration through membranes, Desalination 149 (2002) 417–422.

[3] J.G. Jacangelo, S.S. Adham, J.M. Laîné, Mechanisms of cryptosporidium, giardia and MS2 virus removal by MF and UF, J. AWWA 7 (1995) 107–121.

[4] P. Brown, Assessing the molecular weight cut-off value of UF membranes, Membr. Technol. 61 (1995) 7–9.

[5] K.J. Kim, A.G. Fane, R. Ben Aim, M.G. Liu, G. Jonsson, I.C. Tessaro, A.P. Broek, D. Bargeman, A comparative study of techniques used for porous membrane characterization: pore characterization, J. Membr. Sci. 87 (1994) 35–46.

[6] C. Causserand, P. Aimar, C. Vilani, T. Zambelli, Study of the effects of defects in ultrafiltration membranes on the water flux and the molecular weight cut-off, Desalination 149 (2002) 485–491.

[7] P. Aimar, M. Meireles, V. Sanchez, A contribution to the translation of retention curves into pore size distributions for sieving membranes, J. Membr. Sci. 54 (1990) 321–338.

[8] W.S. Opong, A.L. Zydney, Diffusive and convective protein transport through asymmetric membranes, AIChE J. 37 (1991) 1497–1510.

[9] K.S. Spiegler, O. Kedem, Thermodynamics of hyperfiltration (reverse osmosis): criteria for efficient membranes, Desalination 1 (1966) 311–326.

[10] W.M. Deen, Hindered transport of large molecules in liquid-filled pores, AIChE J. 33 (1987) 1409–1424.

[11] P. Pradanos, J.I. Arribas, A. Hernandez, Mass transfer coefficient and retention of PEGs in low pressure cross-flow ultrafiltration through asymmetric membranes, J. Membr. Sci. 99 (1995) 1–20.

[12] P. Bacchin, Formation et résistance au transfert d'un dépôt de colloïdes sur une membrane d'ultrafiltration, Thèse de l'Université Paul Sabatier, No. 1743, Toulouse, France, 1994.

[13] P. Bacchin, P. Aimar, V. Sanchez, Influence of surface interaction on transfer during colloid ultrafiltration, J. Membr. Sci. 115 (1996) 49–63.

[14] C. Combe, C. Guizard, P. Aimar, V. Sanchez, Experimental determination of four characteristics used to predict the retention of a ceramic nanofiltration membrane, J. Membr. Sci. 129 (1997) 147–160.

[15] G. Schock, A. Miquel, R. Birkenberger, Characterization of ultrafiltration membranes: cut-off determination by gel permeation chromatography, J. Membr. Sci. 41 (1989) 55–67.

[16] C.M. Tam, T.A. Tweddle, O. Kutowy, J.D. Hazlett, Polysulfone membranes II. Performance comparison of polysulfone-poly(*N*-vinylpyrrolidone) membranes, Desalination 89 (1993) 275–287.

[17] I. Gancarz, G. Pozniak, M. Bryjak, W. Tylus, Modification of polysulfone membranes. 5. Effect of *n*-butylamine and allylamine plasma, Eur. Polym. J. 38 (2002) 1937–1946.

[18] R. Nobrega, H. de Balmann, P. Aimar, V. Sanchez, Transfer of dextran through ultrafiltration membranes: a study of retention data analyzed by gel permeation chromatography, J. Membr. Sci. 45 (1989) 17–36.

[19] C.M. Tam, A.Y. Tremblay, Membrane pore characterization—comparison between single and multicomponent solute probe techniques, J. Membr. Sci. 57 (1991) 271–287.

[20] French Standard NF X 45-103, AFNOR Association Française de Normalisation, 1997.

[21] M. Meireles, A. Bessieres, I. Rogissart, P. Aimar, V. Sanchez, An appropriate molecular size parameter for porous membranes calibration, J. Membr. Sci. 103 (1995) 105–115.

[22] A. Akbari, S. Desclaux, J.C. Remigy, P. Aptel, Treatment of textile dye effluents using a new photografted nanofiltration membrane, Desalination 149 (2002) 101–107.

[23] Handbook of Chemistry and Physics, 58 ed., CRC Press, 1977–1978.

[24] G. Jonsson, P.M. Christensen, Separation Characteristics of Ultrafiltration Membranes, Plenum Press, 1986, pp. 179–190.